

# Rapid ElectroMagnetic Induction profiling for pre-drill risk reduction in water-well siting

---

Louis-Arthaud Donzé-Magnier<sup>1</sup>, Aldric Donzé-Magnier<sup>1</sup> and Frédéric Victor Donzé<sup>1,\*</sup>

\*Corresponding author e-mail: fvd@geonum.com

## Affiliations

<sup>1</sup>Geonum Association

## Abstract

Drilling a productive water well in heterogeneous hillside terrain often comes down to choosing the right spot within a few tens of meters. We describe a rapid electromagnetic induction (EMI) survey designed to guide such a decision. Using a CMD-DUO system at 925 Hz with three coil separations (10, 20, 40 m) and two orientations (HCP/VCP), we profiled ~100 m across an agricultural field above a perennial spring. Apparent conductivity increases systematically toward the western end of the transect, with the deepest configurations showing the strongest contrast. Inversion in EMagPy yields a laterally restricted conductive body at ~8–15 m depth (overall RMSPE < 5%). We interpret this anomaly as a plausible drilling target, consistent with perched saturation or wetter colluvium feeding the downslope discharge, while acknowledging that EMI alone cannot distinguish saturation from clay enrichment. The workflow illustrates how dense, multi-configuration EMI profiling and transparent inversion can reduce pre-drill uncertainty at low cost.

## Keywords

Single-frequency frequency-domain EMI (925 Hz); CMD-DUO; Hydrogeophysics; Water-well siting; 1D inversion (EMagPy)

## Introduction

Groundwater remains the most practical water source for many rural communities and farms, yet drilling a borehole is an expensive gamble. Costs are incurred upfront, while yield, reliability, and water quality only become known once the hole is complete. In hard-rock and hillside settings uncertainty is amplified by lateral discontinuity: aquifers pinch out, fracture zones are narrow, and weathered horizons vary over short distances. A borehole placed thirty meters to the left might have succeeded where one to the right failed (Freeze & Cherry, 1979). Pre-drill investigation cannot guarantee water, but it can shift the odds. The aim is

threefold: identify architectures likely to store and transmit groundwater, rule out unfavorable domains such as clay-rich or saline zones, and bracket a realistic depth window with explicit uncertainty. A staged workflow typically begins with desk study, existing wells, geological maps, topography, then moves to targeted field measurements. Near-surface geophysics fills the gap between sparse point data and provides a spatial framework against which conceptual models can be tested (Ward, 1990; Reynolds, 2011). Electrical and electromagnetic methods are particularly suited to this role because bulk conductivity responds to the very properties that matter for groundwater: clay content, saturation, and pore-water salinity (Binley & Slater, 2020). Electromagnetic induction (EMI) operated in the frequency domain is fast, non-invasive, and well suited to profiling: dense station spacing is practical because no ground contact is required. For well siting, these operational advantages can outweigh the method's well-known limitations, non-uniqueness between conductive clay and saline or saturated horizons, sensitivity to shallow heterogeneity, and vulnerability to cultural noise (Beamish, 2011; Boaga, 2017). Used judiciously, EMI narrows the hypothesis space before committing to slower, more diagnostic techniques such as DC resistivity imaging.

In this context, the CMD-DUO is a practical field choice. It combines large coil separations (10, 20, 40 m) with both horizontal and vertical coplanar configurations, enabling multi-depth apparent-conductivity profiling under good temperature stability and straightforward logistics (Pavoni et al., 2023; GF Instruments, CMD-DUO manual). The present study applies this instrument to a concrete problem: where, within a single agricultural field, should a borehole be drilled to intercept the groundwater system that discharges as a perennial spring some 500 m downslope?

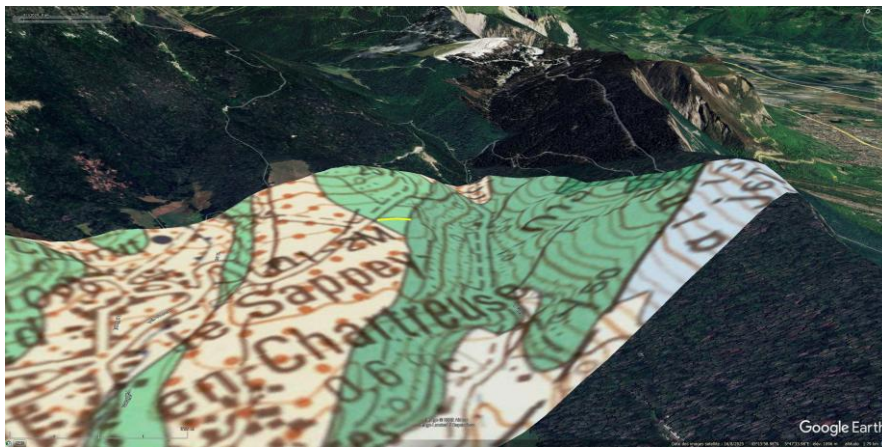
### Study area and hydrogeological context

The survey was designed around two practical questions: where to place the borehole and how deep to drill. The working hypothesis is simple: if the spring marks a focused outlet of a local flow system, then mapping conductivity contrasts upslope may reveal a favorable capture zone. According to BRGM geological mapping (InfoTerre: <https://infoterre.brgm.fr>), the transect lies within unit n1-2M, the so-called Narbonne marls of the Chartreuse area (Lower Cretaceous). This unit comprises marl-dominated intervals alternating with argillaceous limestones. Such lithological contrasts typically generate strong permeability differences: fractured, locally karstified carbonate beds transmit water efficiently, whereas marly layers impede vertical drainage and promote perched saturation and lateral flow. Springs commonly occur where this lateral component encounters a slope break or a structural discontinuity (Ford & Williams, 2007; Goldscheider & Drew, 2007).

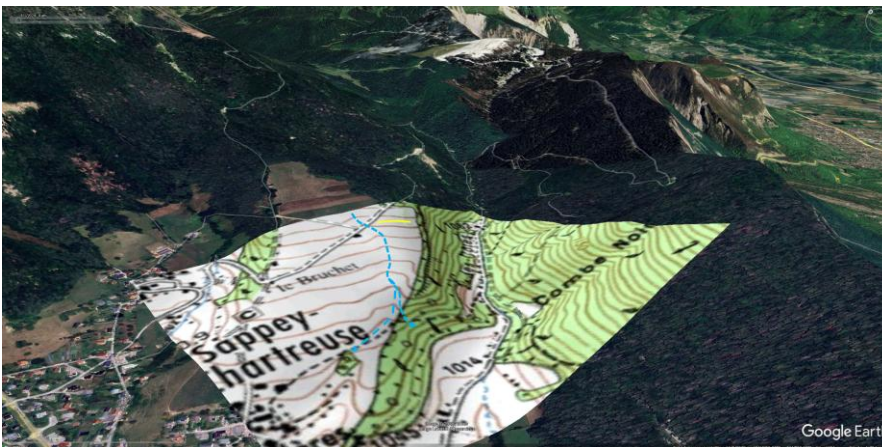
The CMD-DUO transect was therefore positioned to cross expected lateral variability in superficial cover thickness, clay content, and moisture, the properties most likely to govern conductivity contrasts in this setting. A ~100 m profile was surveyed across the field (Figure 1a), connecting the upslope agricultural land to the area above the spring outlet (Figure 1c).



(a)



(b)



(c)

**Figure 1. Site context and geological setting.** (a) Oblique satellite view showing the ~100 m EMI transect (yellow line) across the field. (b) BRGM geological map (InfoTerre) showing the transect within unit n1-2M (Narbonne marls; Lower Cretaceous). Geological attribution follows the BRGM Grenoble sheet and explanatory notice (BRGM, 1978). (c) Perennial spring located ~500 m downslope, interpreted as a discharge point of the local groundwater system (dashed line). Map source: BRGM InfoTerre.

## Methods

### Field acquisition

Data were acquired with a GF Instruments CMD-DUO frequency-domain electromagnetic system operating at 925 Hz. The profile was materialized using flags planted every 5 m, yielding 21 stations over approximately 100 m (Figure 2a). This dense spacing was chosen to capture metre- to decametre-scale lateral changes in cover thickness, clay content, and moisture distribution. At each station we recorded six readings: three coil separations (10, 20, 40 m) in two configurations (HCP and VCP, labelled "Hi" and "Lo" in CMD-DUO terminology; see Figure 2b). Increasing coil separation shifts sensitivity toward greater depth, while the two coil orientations provide different vertical weighting functions, together improving discrimination between shallow heterogeneity and deeper conductive features (McNeill, 1980). Cable midpoints were pre-marked to maintain constant geometry from station to station. Consistent instrument alignment, near-constant coil height, and adequate stabilization time were maintained throughout. Cultural noise was minimized by avoiding metallic objects and infrastructure.

The six-configuration bundle also serves as an internal quality check: isolated inconsistencies relative to adjacent stations or across configurations were flagged for review. Apparent conductivity was recorded for all configurations; in-phase data were logged for quality control but are not interpreted further here.

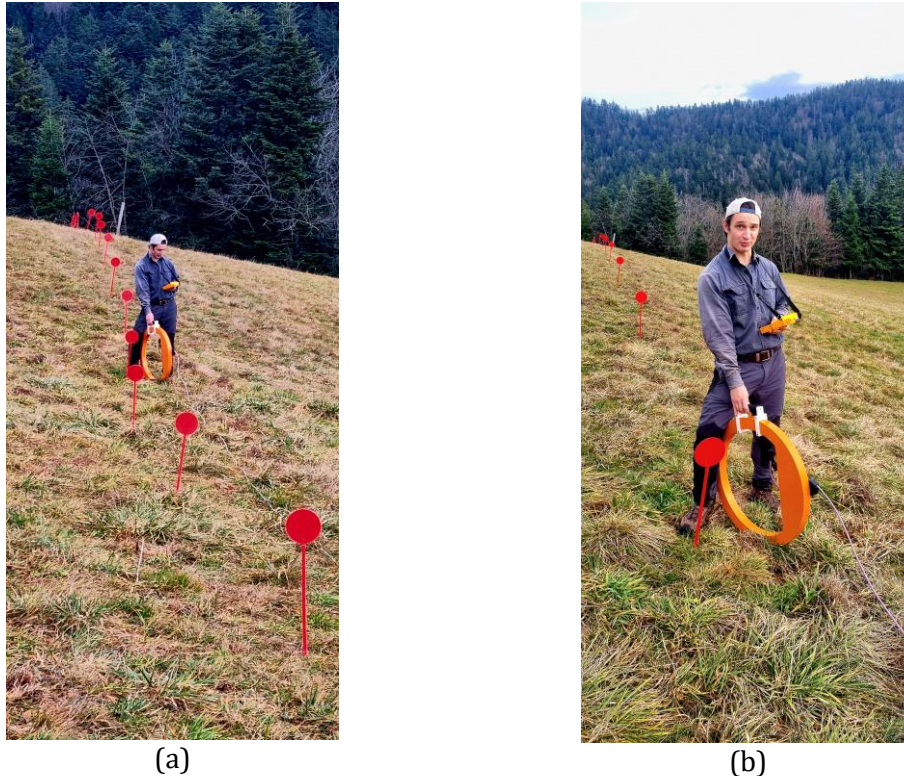


Figure 2. **CMD-DUO acquisition.** (a) Field layout with flags every 5 m (21 stations over ~100 m). (b) Instrument deployment; at each station, six measurements were acquired (three coil separations × two configurations) to provide multi-depth.

### Inversion workflow

The six apparent-conductivity curves were inverted using EMagPy v1.4.2, an open-source platform for forward modelling and 1D inversion of EMI data (McLachlan et al., 2021). Forward response was computed with the cumulative-sensitivity formulation, which performs well under low-induction-number conditions (McNeill, 1980).

Each station was represented as a 1D layered earth with fixed layer interfaces and unknown conductivities. The starting model comprised 100 layers of 0.5 m thickness (40 m total depth) and a uniform conductivity of 20 mS/m. This fine discretization avoids imposing arbitrary interfaces; vertical complexity is instead controlled by regularization. We applied L2 (Tikhonov-type) smoothness regularization to stabilize the inherently non-unique inverse problem (Hansen, 1992). A vertical smoothness weight of 0.02, close to the L-curve elbow, was selected after testing a range of values; lateral smoothing was set to zero so that each station was inverted independently. Optimization used the L-BFGS-B solver with positivity constraints on conductivity (25 iterations maximum). The displayed section is therefore a compilation of independent 1D models rather than a true 2D inversion. As expected for EMI, resolution degrades with depth below the main sensitivity range; deep conductivity values become increasingly controlled by regularization and the starting model.

## Results

### Apparent conductivity profiles

Apparent conductivity shows clear lateral organization along the profile (Figure 3). For clarity, the abscissa is plotted with 0 m at the western end, matching field orientation. All configurations record a systematic decrease from west to east, but the deeper-sounding settings (HCP20, HCP40) display the strongest contrast, suggesting that the main anomaly is not confined to the shallow soil. In the western sector (0–20 m), conductivities are highest, typically 45–60 mS/m for intermediate configurations; HCP40 also shows elevated values compared with the rest of the line. Moving eastward, apparent conductivity decreases progressively, reaching 30–40 mS/m in the eastern sector. Two features are reproducible across configurations: a pronounced break in HCP20 around 35–45 m, and a step-like change in HCP40 near 30 m, consistent with a lateral transition at depth.

### Inversion outcome

The inverted section reveals a laterally restricted conductive domain centered at intermediate depth (~8–15 m) that intensifies toward the western end of the profile (Figure 3b). Overall agreement between observed and predicted responses is high, with an overall RMSPE below 5% (Figure 4). Misfit varies by configuration: HCP10 and HCP40 show the lowest residuals, whereas VCP40 and HCP20 are slightly noisier, plausibly because deeper configurations are more sensitive to violations of the 1D assumption where lateral heterogeneity is present. Importantly, the inversion reproduces the main lateral trend consistently across all configurations, supporting the interpretation of a real subsurface contrast rather than a configuration-specific artefact.

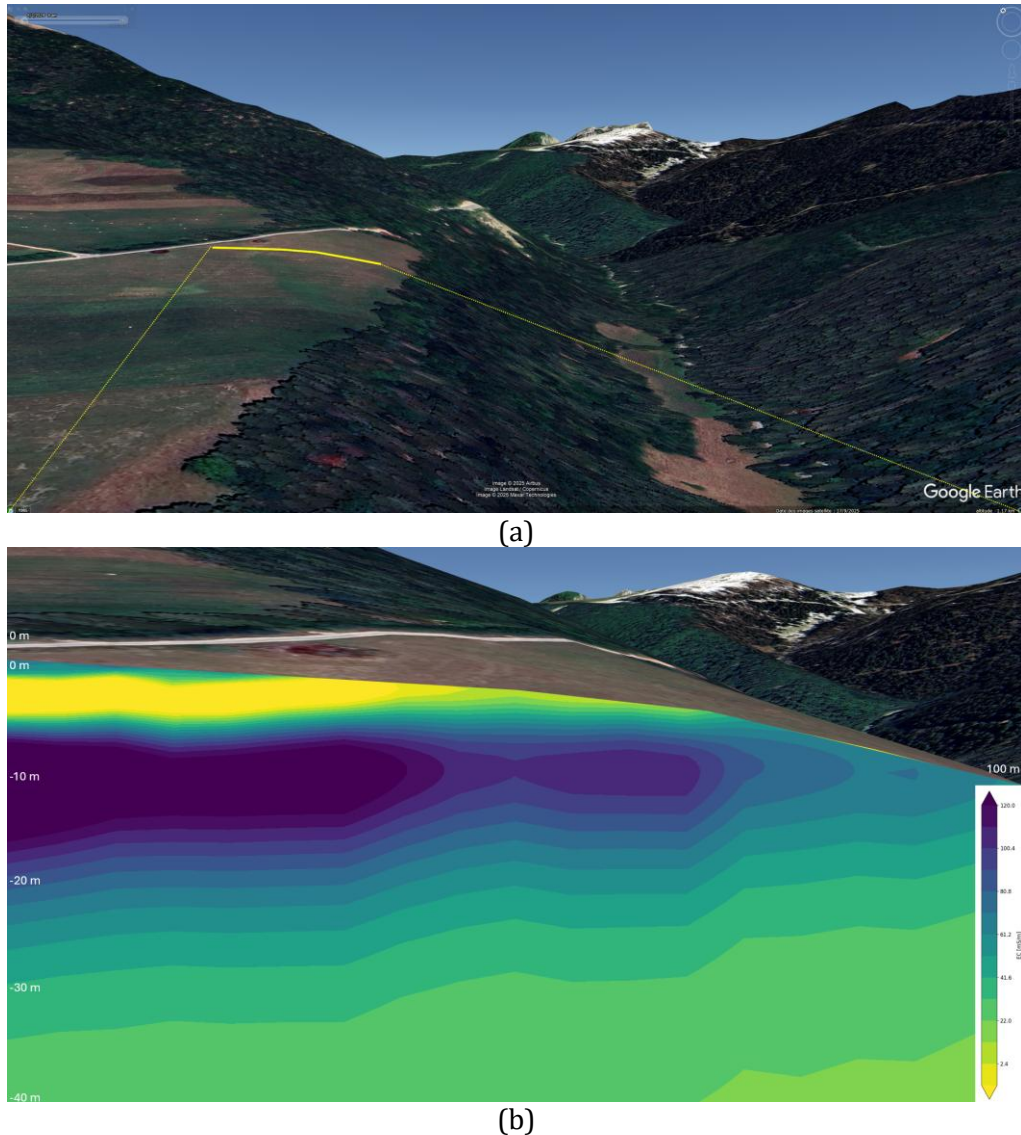


Figure 3. **Apparent conductivity and inverted conductivity section.** (a) Site view with transect location. (b) Conductivity section from independent 1D inversions (EMagPy) to 40 m depth. Note: 0 m corresponds to the western end of the field. The main conductive domain is laterally restricted and centered at ~8–15 m depth beneath the western sector.

### Discussion and conclusions

The profiles and inversion together provide a coherent, field-scale constraint for well siting. The most conductive sector lies in the western part of the line (roughly 0–20 m on the plotted axis, with a broader transition up to ~40 m), where the inversion locates a conductive body centered at ~8–15 m depth.

What does this anomaly represent? Conductivity in EMI data typically increases with clay fraction, saturation, and dissolved solids. The anomaly may therefore reflect a wetter horizon, perched water above a low-permeability marl, saturated colluvium, or conductive pore water in a fracture zone, or a clay-rich interval that remains conductive even at moderate saturation. EMI alone does not resolve transmissivity, so the interpretation remains

conditional. Nevertheless, the anomaly is compatible with the mapped geology. The transect lies within the Narbonne marls, a unit expected to contain low-permeability intervals that promote perched saturation and lateral drainage. In such carbonate-marl sequences, lateral flow above marly barriers and discharge at slope breaks are common spring-forming mechanisms (Ford & Williams, 2007; Goldscheider & Drew, 2007). Under this model, the western conductive sector plausibly corresponds to thicker or wetter cover and may represent the upslope continuation of the system feeding the downslope spring.

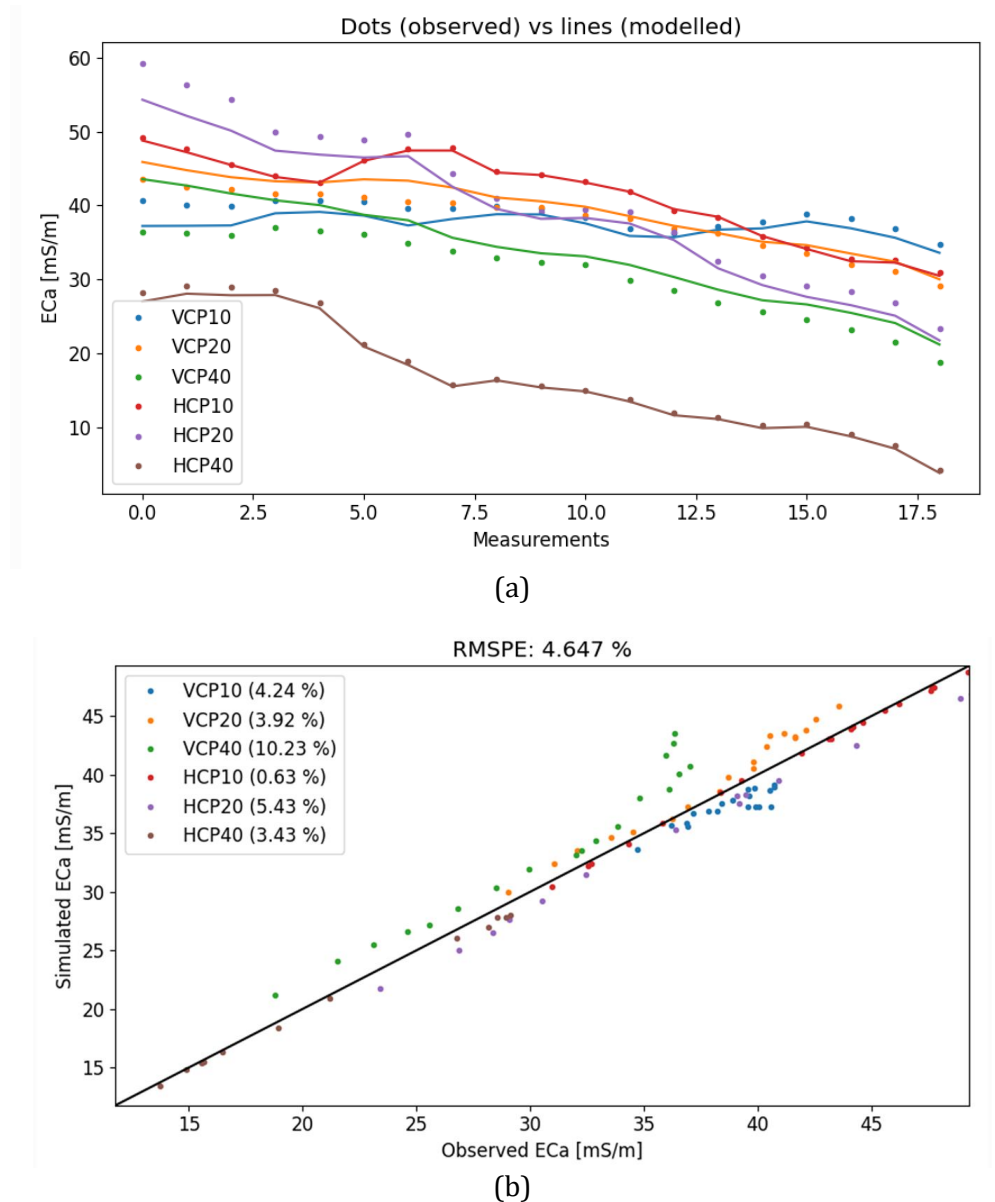


Figure 4. **Data-model agreement.** (a) Residuals (observed minus predicted) for each configuration along the transect. (b) RMSPE by configuration and overall, used to assess inversion stability.

Comparable studies support the practical value of multi-configuration EMI for hydrogeological targeting when combined with transparent inversion and conservative interpretation. Rejiba et al. (2018) demonstrate how such data can resolve the geometry of conductive bodies in alluvial settings; EMagPy provides a documented, reproducible framework for translating multi-configuration EMI into conductivity–depth models with explicit fit diagnostics (McLachlan et al., 2021).

## Conclusions and operational recommendation

If the objective is to maximize the probability of intersecting a saturated horizon related to the downslope discharge, the most defensible first drilling target lies within the western high-conductivity sector. An initial depth window of ~10–15 m is reasonable, with the option to deepen depending on drilling response. To reduce the remaining ambiguity between "wet" and "clayey", a short confirmatory step, a focused ERT line across the anomaly, or shallow augering, would strengthen the drilling decision at modest additional cost. Dense EMI profiling does not replace such diagnostics, but it does provide a rational basis for deciding where to deploy them.

## References

- Beamish, D. (2011). Low induction number, ground conductivity meters: A correction procedure in the absence of magnetic effects. *Journal of Applied Geophysics*, 75, 244–253.
- Binley, A., & Slater, L. (2020). *Resistivity and Induced Polarization: Theory and Applications to the Near-Surface Earth*. Cambridge University Press.
- Boaga, J. (2017). The use of FDEM in hydrogeophysics: A review. *Journal of Applied Geophysics*, 139, 36–46.
- BRGM. (1978, 2nd ed.). Notice explicative, Carte géologique de la France (1/50 000), feuille Grenoble (n°772). BRGM, Orléans.
- Ford, D. C., & Williams, P. (2007). *Karst Hydrogeology and Geomorphology*. Wiley.
- Freeze, R. A., & Cherry, J. A. (1979). *Groundwater*. Prentice-Hall.
- GF Instruments. CMD-DUO User Manual / Technical Documentation.
- Goldscheider, N., & Drew, D. (Eds.). (2007). *Methods in Karst Hydrogeology: A Practical Guide*. Taylor & Francis.
- Hansen, P. C. (1992). Analysis of discrete ill-posed problems by means of the L-curve. *SIAM Review*, 34(4), 561–580.
- McLachlan, P., Blanchy, G., & Binley, A. (2021). EMagPy: Open-source standalone software for processing, forward modeling and inversion of electromagnetic induction data. *Computers & Geosciences*, 146, 104561.

Donzé-Magnier L-A., Donzé-Magnier A.& Donzé F-V., **Rapid ElectroMagnetic Induction profiling for pre-drill risk reduction in water-well siting**, Geonum Ed.: ISRN GEONUM-NST--2025-03--ENG, 9 pages, 2025. DOI: 10.5281/zenodo.18048063

McNeill, J. D. (1980). Electromagnetic terrain conductivity measurement at low induction numbers (Technical Note TN-6). Geonics Ltd.

Pavoni, M., Boaga, J., Carrera, A., Urbini, S., de Blasi, F., & Gabrieli, J. (2023). Combining Ground Penetrating Radar and Frequency Domain Electromagnetic Surveys to Characterize the Structure of the Calderone Glacieret. *Remote Sensing*, 15(10), 2615.

Rejiba, F., Schamper, C., Chevalier, A., Deleplancque, B., Hovhannissian, G., Thiesson, J., & Weill, P. (2018). Multiconfiguration electromagnetic induction survey for paleochannel internal structure imaging: a case study in the alluvial plain of the River Seine, France. *Hydrology and Earth System Sciences*, 22, 159–170.

Reynolds, J. M. (2011). *An Introduction to Applied and Environmental Geophysics* (2nd ed.). Wiley-Blackwell.

Ward, S. H. (Ed.). (1990). *Geotechnical and Environmental Geophysics*. Society of Exploration Geophysicists.